Chemical Engineering Journal 150 (2009) 231–236

Contents lists available at ScienceDirect

Chemical Engineering Journal

journal homepage: www.elsevier.com/locate/cej

A reactor for the study of homogeneous processes using laser radiation energy

V.N. Snytnikov [a], T.I. Mischenko [a], Vl.N. Snytnikov [a], I.G. Chernykh [b,*]

[a] Boreskov Institute of Catalysis SB RAS, Lavrentjeva ave. 5, Novosibirsk, 630090, Russia
[b] Institute of Computational Mathematics and Mathematical Geophysics SB RAS, Lavrentjeva ave. 6, Novosibirsk, 630090, Russia

ARTICLE INFO

Article history:
Received 29 September 2008
Received in revised form 12 February 2009
Accepted 23 February 2009

Keywords:
Ethane pyrolysis
Ethylene
Laser
Radiation

ABSTRACT

A flow reactor with the reactants heated by continuous CO_2 laser radiation is proposed for studying the gas phase homogeneous reactions. Ethane pyrolysis yielding ethylene is considered as an example of such chemical process. For this process, a mode of 'energetic catalysis' is feasible, where increasing energy absorption in the volume is related with the increased content of target product. The mode of 'energetic catalysis' was implemented at transformation of laser energy into thermal power using the sensitization properties of ethylene. In the pyrolysis reaction zone, temperature measurements were made for a gas mixture in the laser radiation field with a power density up to 10^2 W/cm^2. The walls and windows were isolated from the high-temperature zone by argon feeding and configuration of the reactor. Three-dimensional calculation of the gas-dynamic reactants flows and their mixing made with the FLUENT software package showed the presence of the modes where reaction zone with a high content of C_2 hydrocarbons is localized in the center of reactor, which was confirmed by experiments. High values of ethane conversion up to 80 vol.% were obtained at nearby 53% selectivity for ethylene.

1. Introduction

Endothermic chemical processes are carried out in the reactors with energy input to the reaction zone. Such reactors are distinguished by the energy source, which can be represented by electric arc [1–4], heat from combustion of a part of feedstock with oxygen in reactor [5], cyclic heating of catalyst [6], inert gas at a high-temperature [7], or reactor tubes [8,9]. A wide variety of the heating methods and endothermic chemical processes implies special-purpose designs of chemical reactors: turbulent flow reactors, reactors with shock waves in a tube, and plasma reactors [10–14].

The above-listed reactors are used to run the endothermic chemical processes like cracking and pyrolysis of hydrocarbons. However, the efficient use of delivered energy still remains a topical problem. For instance, when acetylene is obtained from methane by electric arc heating, only 30% of supplied energy can be put into the energy of bond cleavage and formation of new chemicals bond. In this process, high rates of energy input provide fast heating of the reactants, which leads to a temperature gradient in the reaction zone up to 100–200 K/mm. However, in this case, spatial heterogeneity of the medium is observed, which decreases the selectivity for target products due to a pronounced temperature dependence of chemical reaction constants.

Another problem is related with optimization of reactants residence time in the reaction zone to prevent the involvement of target products in secondary reactions. Thus, thermal dehydrogenation of C_2–C_4 hydrocarbons yielding ethylene and propylene is characterized by high reactivity of these products at the temperatures of pyrolysis. This imposes specific constraints on the reactor design.

The use of laser radiation for heating the reaction medium makes possible the direct input of energy to the gas with the power density of 10^2 W/cm^2, which exceeds by one and a half—two orders of magnitude the values attained in reactors with metal walls. This circumstance allows decreasing the time of reactants' pyrolysis to milliseconds. Possibility of using laser energy as a powerful energy source for the chemical reactors gives impact to the scientists for studying endothermal chemical processing. There are many different trends initiated in gas-core reactions studying [15–30], preparation of catalysts [20], polymer films synthesis [22], heat-and-mass transfer, interaction between laser radiation and gas medium, effect of laser radiation energy on chemical reactions equilibrium [24–28] during 70–80 years of twenties century. At the power density below 10^5 to 10^6 W/cm^2, energy absorption and reaction occurrence at atmospheric and higher pressures follow the thermal mechanism [29]. A necessary condition for application of laser radiation is that the reaction medium comprises a component which absorption spectrum contains the bands coinciding with the region of laser generation. In this case, the absorbed energy of laser radiation is transmitted at collisional relaxation to the reac-

* Corresponding author. Tel.: +7 383 3309665; fax: +7 383 3308783.
E-mail addresses: snyt@catalysis.ru (V.N. Snytnikov), snyt@catalysis.ru (Vl.N. Snytnikov), chernykh@ssd.sscc.ru (I.G. Chernykh).

1385-8947/$ – see front matter © 2009 Elsevier B.V. All rights reserved.
doi:10.1016/j.cej.2009.02.028

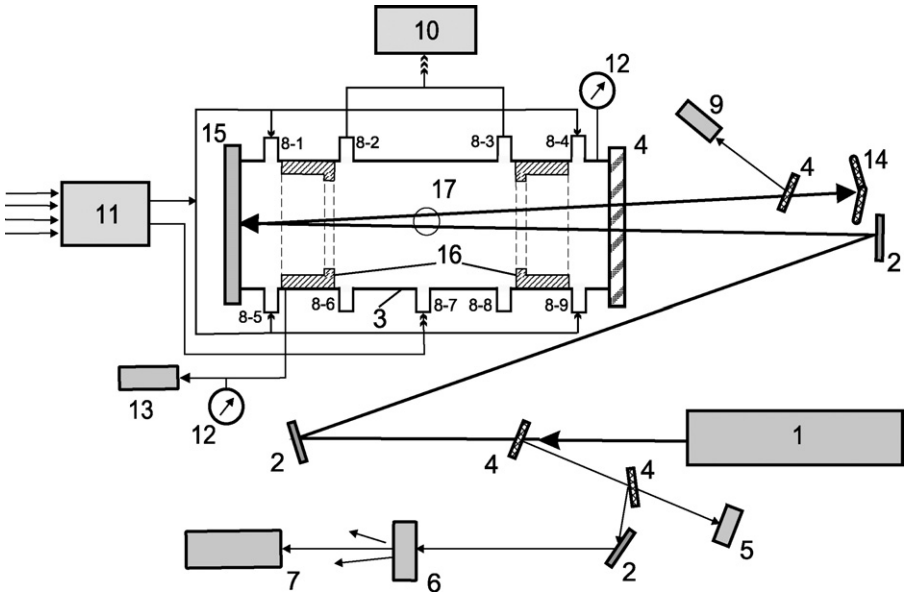

Fig. 1. Schematic diagram of the wall-less reactor for ethane pyrolysis. 1. CO_2 laser unit. 2. Mirrors of the optical route. 3. Reactor. 4. Optical windows (ZnSe). 5. Radiation power meter LM-2 unit. 6. Diffusing window (NaCl). 7. InfraLUM FT-801 Fourier transform spectrometer unit. 8-1, 4, 5, 9—Ar inputs. 8-2, 3—Gas mixture output. 8-7—Ethane–ethylene mixture input. 8-6, 8—Closed plugs. 9. Radiation power meter TI-3 unit. 10. Chromatographs Crystal 2000M and LHM-80MD units. 11. UFGP-4 gas flow former. 12. Vacuum manometers. 13. Forevacuum pump unit. 14. CO_2 laser energy absorber. 15. Al mirror of the reactor. 16. Diaphragms.

tion medium, thus heating it. When studying the process kinetics, it is important to provide the gas-phase occurrence of the reactions. A necessary thermal insulation of the reaction zone can be provided by buffer gas supercharging at the sites of laser radiation input and by a relatively cold mixture of reactants in the rest near-wall region of convectively cooled reactor. For cylindrical geometry, such mode can be implemented via a smaller section of laser beam as compared to reactor section.

This work presents results of the study of a flow reactor with laser input of energy for endothermic reactions exemplified by ethane pyrolysis. The reactions were conducted under homogeneous conditions at atmospheric pressure in the reactor with the reaction mixture components heated by the laser energy flux delivered directly into the gas. Ethylene, being among the main reaction products, served as the laser energy absorber. This created the mode of 'energetic catalysis'. Here, increasing energy absorption in the volume is related with the increased content of the reaction product.

Pilot prototype of the reactor was tested with using of FLUENT software package. There was different tests with geometry modifications and different mass flow rates of reactants.

2. Experimental

2.1. Experimental procedure

Fig. 1 shows a general scheme of experimental setup for the study of pyrolysis of C_2–C_3 hydrocarbons with temperature measurements. A continuous CO_2 laser with the maximum power W_0 = 130 W (1) was used as the energy source. The radiating power was controlled using a clarified ZnSe plate (4) and an LM-2 power meter (5) with the time resolution 2.5 s. A part of radiation was tapped by a GaAs plate (4) and through a diffusing NaCl plate (6) was directed to the inlet of InfraLUM FT-801 Fourier transform spectrometer (7) that allows recording the lasing spectrum with 0.5 cm^{-1} resolution at characteristic time of nearby 10 s. Diameter of the wave beam at the reactor inlet was 12 mm.

Using a system of copper mirrors (2), laser radiation was delivered into reactor (3) at a small angle to longitudinal axis through the clarified ZnSe plate. At the second face of the reactor, an Al mirror (9) was mounted to direct the transmitted radiation back into reactor. The part of radiation unabsorbed in reactor was sent through a dividing KCl plate to a TI-3 power meter (9) with the time resolution of 10 s and recording range of 0.1–100 W. Chemical analysis of the initial mixture of gases and reaction products for the content of C_1–C_4 hydrocarbons and H_2 was made chromatographically. Sampling was performed with a syringe at the reactor outlet and, in the absence of radiation, through the reactor channels (8-1/9) at any point of the chamber volume.

A four-channel UFGP-4 flow former (11) was used to mix the initial gases and specify their flow rate through the reactor. Gas pressure at the reactor inlet and outlet was controlled by indicating vacuum manometers (12). Reaction products were removed by a 2NVR-0.1D vacuum pump (13), with the outlet pressure maintained at 0.95 atm. Pressure of the gas mixture at the reactor inlet was 1 atm.

2.2. Reactor design and temperature diagnostics

A schematic diagram of reactor indicating the temperature gauges layout is displayed in Fig. 1. Reactor is made of a quartz tube with the inner diameter 20 mm and length 70 mm. Four inlets (8-1, 4, 5, 9) were used for Ar feeding into reactor to protect optical parts and decrease the effective length of the reaction zone. For the same purpose, stainless steel diaphragms (16) with straight-through diameter 12.5 mm were mounted in the chamber. The ethane–ethylene mixture was fed into reactor via inlet (8-7) in the central section. Four inlets (8-2, 3, 6, 8) symmetric about the central axis were used to remove a mixture of reaction products with argon. In the same section, with a 90° shift, temperature gauges (17) were placed: a heat-insulated Mo plate 50 μm in thickness and 2.5 mm in diameter—for pyrometric measurements, or a spiral thermistor made of copper wire 70 μm thick, with coil diameter 3 mm and 0.4 Ωimpedance. The axis of six-turn copper spiral and the plane of molybdenum gauge are oriented along the laser beam axis. In the same section with the gauges, a thermocouple is mounted in the chamber to measure the gas temperature at a distance of 0.5–1 mm from the lateral wall of reactor.

To measure the brightness temperature and calculate the absolute temperature, we used an EOP-66 optical pyrometer with effective wavelength 0.655 μm. The operating temperature range of pyrometer was 800–10,000 °C. The total rated measurement error for the luminance temperature in sub-range 800–1400 ° C did not exceed ±8 °C. A correction for determination of the absolute (true) temperature related with the value of spectral radiative ability of Mo in the temperature range 800–1000 °C, $\varepsilon \approx 0.4$, was equal to +(45–60) °C. Irradiation of the pyrometric gauge was recorded through the quartz wall of reactor using a rotary mirror at a distance of nearby 2 m.

There are several reasons for choosing the copper thermistor for temperature measurements. First, the temperatures under consideration range from 300 to 1000 °C. Second, thermistor should not affect the processes in reactor. Third, the thermistor material should be resistant to CO_2 laser radiation with power density up to 200 W/cm^2 and have a low level of radiation absorption. It is necessary also to provide time resolution of ca. 1 s and the possibility of operation with standard measuring equipment.

2.3. The mathematical model

The mixing of gas flows in the 3D reactor geometry was calculated with the FLUENT program package [30]. For all flows, FLUENT solves conservation equations for mass and momentum. The equation for conservation of mass, or continuity equation, can be written as follows:

$$\frac{\partial \rho}{\partial t} + \nabla \cdot (\rho \vec{v}) = S_m \quad (1)$$

Eq. (1) is the general form of the mass conservation equation and is valid for incompressible as well as compressible flows. The source S_m is the mass added to the continuous phase from the dispersed second phase and any user-defined sources.

Conservation of momentum in an inertial (non-accelerating) reference frame is described by [31]:

$$\frac{\partial}{\partial t}(\rho \vec{v}) + \nabla \cdot (\rho \vec{v}\,\vec{v}) = -\nabla p + \nabla \cdot (\bar{\bar{\tau}}) + \rho \vec{g} + \vec{F} \quad (2)$$

where p is static pressure, $\bar{\bar{\tau}}$ is is the stress tensor (described below), and $\rho \vec{g}$ and $\vec{F}$ are the gravitational body force and external body forces (e.g., that arise from interaction with the dispersed phase), respectively. $\vec{F}$ also contains other model-dependent source terms such as porous-media and user-defined sources. The stress tensor $\bar{\bar{\tau}}$ is given by

$$\bar{\bar{\tau}} = \mu[(\nabla \vec{v} + \nabla \vec{v}^{\,T}) - \frac{2}{3}\nabla \cdot \vec{v} I]$$

where μ is the molecular viscosity, I is the unit tensor, and the second term on the right hand side is the effect of volume dilation. When you choose to solve conservation equations for chemical species, FLUENT predicts the local mass fraction of each species, Y_i, through the solution of a convection–diffusion equation for the ith species. This conservation equation takes the following general form:

$$\frac{\partial}{\partial t}(\rho Y_i) + \nabla \cdot (\rho \vec{v} Y_i) = -\nabla \cdot \vec{J}_i + R_i + S_i \quad (3)$$

where R_i is the net rate of production of species i by chemical reaction and S_i is the rate of creation by addition from the dispersed phase plus any user-defined sources. An equation of this form will be solved for $N-1$ species where N is the total number of fluid phase chemical species present in the system. Since the mass fraction of the species must sum to unity, the N th mass fraction is determined as one minus the sum of the $N-1$ solved mass fractions. More detailed information about FLUENT solver available in FLUENT documentation at [30]. In our computational experiments we use laminar flow model because Re number in our calculations is very small. In flow calculations, we used the ideal gas approximation and took into account energy transfer, full multicomponent diffusion of the gas mixture, temperature, viscosity of the mixture components, and its temperature dependence. Mass flow rates of gases at the inlets were specified as boundary conditions, with pressure in the reactor volume taken equal to 1 atm. In the numerical model, geometrical dimensions of reactor corresponded to those of the pilot sample. There was approx. 20 numerical experiments for the purpose of finding optimal reactants flow in reactor. The range of mass flow rate of ethane–ethylene mixture is from 1.05 to 2.2 L/h with mass fraction of C_2H_4 from 30% to 40%. The range of mass flow rate of Ar is from 0.6 to 4.75 L/h.

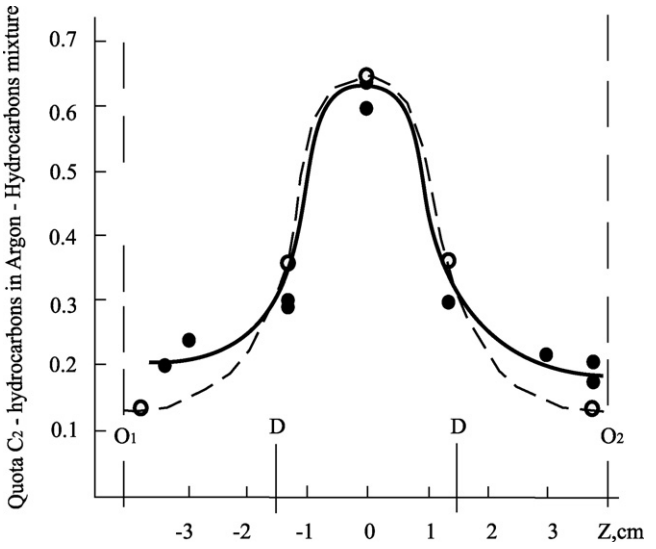

Fig. 2. Distribution of hydrocarbons over the length of reactor in the experiments. O1 and O2—reactor faces, D—diaphragm boundaries in the reaction zone. Dark points—experimental data. Hollow points—calculated data obtained with the FLUENT software.

3. Results

3.1. Formation of gas flows in the reactor—measurement and calculation

In the experiments, total flow rate of argon was set at 3 L/h, and that of the ethane–ethylene mixture—at 1.7 L/h, with the 30% content of ethylene. Mixing of the gas flows was studied at 20 ° C and atmospheric pressure. For the reactor with diaphragms, the fraction of hydrocarbons near the reactor faces was found to be 17%. The axial distribution of hydrocarbons in reactor in the Ar–C_2H_6–C_2H_4 mixture is shown in Fig. 2. Dark points correspond to experimental measurements. One may see that in the central part of reactor the fraction of hydrocarbons makes up 60% and far exceeds their amount near the face walls.

The problem of gas flow mixing was solved numerically using the FLUENT software package for different modes of gas delivery and discharge. Flow rates of argon, ethane and ethylene were set similar to the experiments. For the reactor with diaphragms (16) and shut-off outlet channels 8-6 and 8, calculation gave the 7% fraction of ethane–ethylene mixture near the reactor faces (Fig. 3). The gas flow distribution is shown in the steady-state mode 300 s after the onset of gas feeding. A region with elevated content of hydrocarbons is located in the center of reactor, the C_2H_6–C_2H_4 amount in the region attaining 60% according to this calculation. In Fig. 2, experimental points of C_2 hydrocarbons distribution in the reactor volume are supplemented with the calculated values, which are

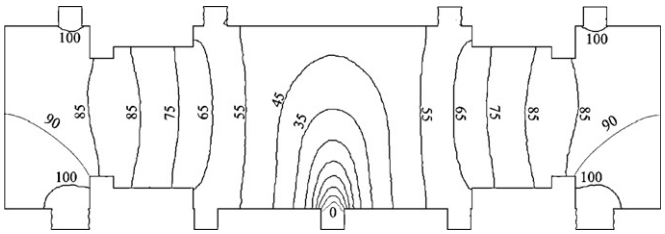

Fig. 3. Distribution of weight fractions of argon in the mixture at 20 ° C and atmospheric pressure for the reactor with diaphragms. Calculation was made using the FLUENT program. Ethane–ethylene mixture with a 30% content of ethylene was fed via the central channel with the total flow rate 1.7 L/h, and argon—via four side inlets with flow rate 3 L/h. The distributions corresponds to the steady-state flow obtained in 300 s.

indicated by hollow points. As follows from this plot, there is a good agreement between the experiment and numerical modeling data.

Flow behavior was studied numerically at high temperatures, with the ethane–ethylene mixture fed at 1050 K and argon at 298 K. At that, chemical reactions and heat abstraction to the reactor walls were not taken into account. The calculation shows that reactor faces are insulated by buffer gas from the reaction zone (Fig. 4). Argon, virtually without hydrocarbon mixture, occupies the region right up to the diaphragm boundaries. For initial mixture in the central zone of reactor, no more than 10% dilution with argon was noted. Presumably, such calculation results are caused by more than a three-fold drop in the density of ethane–ethylene mixture in the central zone at $T = 1050$ K, which is necessary to satisfy the $P \approx 1$ atm condition in the reactor volume. In this case, to retain the mass flow rate of the mixture, flow rate should increase accordingly. Note also that at 1050 K viscosity of the reaction mixture approaches the viscosity of cold argon. In real experiments, gas was heated by radiation in the near-axial region of reactor. As shown by temperature measurements in the experiments with radiation, near-wall temperature of gas in the central zone of reactor did not exceed 380 K, which excludes the occurrence of reactions on the surface.

3.2. Ethane pyrolysis at atmospheric pressure and temperatures below 1000 °C

Dehydrogenation of ethane yielding ethylene was performed with the initial ethane–ethylene mixture at a 30% content of ethylene. Main products of pyrolysis were C_2H_4, CH_4 and H_2. C_3H_6 and C_2H_2 accounted for no more than 1 and 4 vol.%, respectively. Power of continuous CO_2 laser was varied over the range of 50–75 W.

Fig. 5 shows the temperature dependence of ethane conversion. Here, the data obtained with thermistor are denoted as TR, and data of pyrometer—as PD. In the region of 600 °C, ethane conversion makes up only several percents and gradually increases to 80% as the temperature is raised to 850 °C.

Changes in the composition of ethane–ethylene mixture with temperature are presented in Fig. 6, which shows the contents

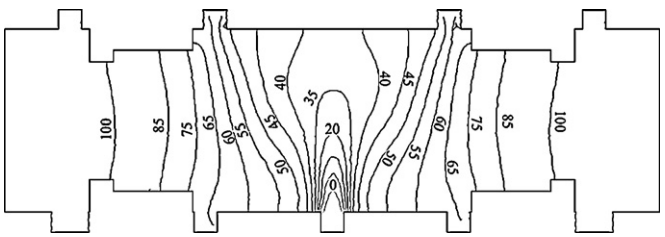

Fig. 4. Distribution of weight fractions of argon in the mixture for the reactor with diaphragms at atmospheric pressure; temperature of argon 298 K, temperature of hydrocarbons mixture 1050 K.

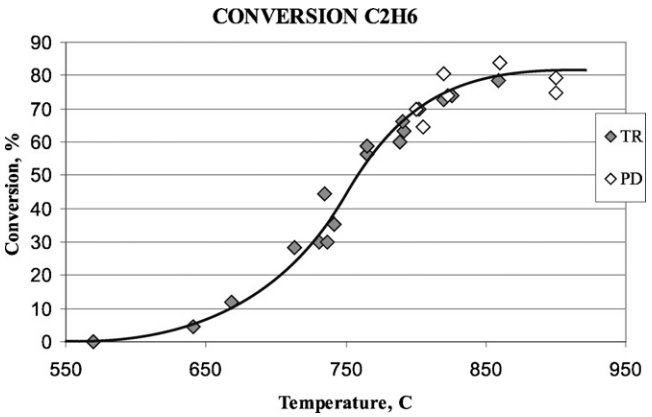

Fig. 5. Temperature dependence of ethane conversion. Initial mixture: C_2H_6—70 vol.%, C_2H_4—30 vol.%. TR—thermistor measurements. PD—optical pyrometer measurements.

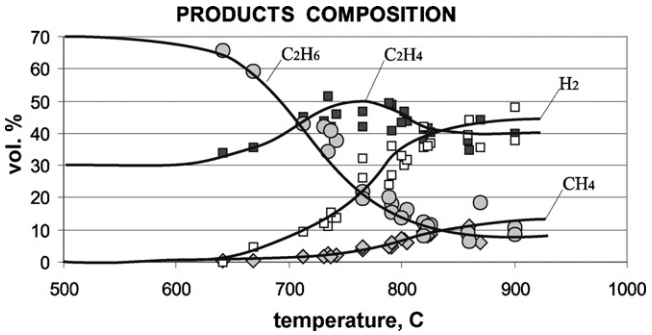

Fig. 6. Changes in the reaction mixture composition with temperature.

of ethane, ethylene, methane and hydrogen in the reaction products. Hydrogen and methane appeared at 650 °C. In the range of 650–900 °C, the H_2 amount attained 40–45% at temperatures above 830 °C. Minute amounts of methane were recorded to the point of 750 °C. As the temperature was raised, the fraction of methane in the reaction products increased, and at 840 ° C its content attained 13 vol.%. The ethylene content passes a maximum with the value of ca. 50 vol.% at 750–780 °C.

4. Discussion

The main method of ethylene production is a pyrolysis of oil distillates or pyrolysis of low paraffin hydrocarbons with water vapors in pipe furnace at 750–900 ° C [32–34]. For example, ethylene yield is 15–25% for the pyrolysis of gas-oil, ethylene production is going up to 50% for the pyrolysis of light alkanes (ethane, propane, butane). There are different ways of processing of hydrocarbons with different organization of catalysts bed [35]. There are many researches of direct conversion of methane to C_2hydrocarbons by oxidative coupling of methane in progress [36–44]. The ethylene yield for this mechanism is 25% with methane conversion less than 20%. The most clean ethylene is made by catalytic dehydration of ethanol at 400–450 ° C [45]. The main description of these methods is a presence of heterogeneous processes on heated surfaces that brings the synthesis of waste products, carburization of pipes and catalysts surfaces with deactivation of catalysts. Our method provides process of ethylene production in homogeneous gas-phase conditions at atmosphere pressure without any diluents. Products variety was limited by CH_3, C_2H_4, C_2H_2, C_3H_6, H_2. There are no heavy organic products were detected on the reactor walls.

Experimentally founded that thermal dehydrogenation of ethane under laser radiation can be initiated if the minimum fraction of ethylene in the reaction mixture exceeds 6 vol.%. A lower content of $C_2H_4$is insufficient for heating the reactants to pyrolysis temperatures at radiating power up to 90 W. No provision was made in the reactor for thermal insulation of the walls, so the convective heat removal through the walls was essential. Reactants' consumption corresponds to the laser radiation power delivered to reactor and to the contact time [46], which characterizes the dwell of reactant in the laser beam field. Experimental measurements and results of numerical modeling demonstrated that near the reactor faces the content of C_2hydrocarbons was 17% and 12%, respectively. Taking into account the 30% content of ethylene in the initial ethane–ethylene mixture, C_2H_4concentration below 6% is insufficient for heating the mixture near the windows to the temperature of pyrolysis. Thus, in the near-wall region of reactor faces, conditions at which chemical reactions can proceed are absent. The temperatures of external surface of reactor faces measured in the experiments did not exceed 120 °C.

In the central part of reactor, there formed a region of argon–C_2 hydrocarbon mixture with predominant content of C_2H_6–C_2H_4, its amount ranging from 45 to 70 vol.%. The highest concentration of C_2 hydrocarbons, 70 vol.%, was observed near the inlet of C_2H_6–C_2H_4 mixture. As the distance to the inlet channel increased, the fraction of C_2 hydrocarbons decreased, its value making up 45 vol.% at the diaphragm boundaries. This is clearly seen from the calculated model (Fig. 3).

The experimental data obtained give a large spread in the content of C_2H_6–C_2H_4 in the Ar–hydrocarbon mixture upon variation of the sampling depth. For example, a sample taken via channel 7 at a distance of 4 mm in the reactor volume contained more than 70% of C_2 hydrocarbons. When the distance was increased to 15 mm, the content of C_2 hydrocarbons decreased to 45 vol.%. Thus, in the central part of reactor, C_2H_4 content ranged from 15 to 23 vol.%. This amount of ethylene in the reaction mixture provided heating of the reactants to 1000 K and higher.

5. Conclusion

A flow reactor with laser input of energy providing the homogeneous conditions for chemical process occurrence has been devised for the study of gas-phase reactions. Three-dimensional modeling of the gas flow mixing was made using the FLUENT program package for the reactor with geometrical dimensions corresponding to the pilot sample. A qualitative agreement between the calculated and experimental data was obtained. This confirmed applicability of FLUENT for designing of this type reactors. Formation of the reaction zone in the center of reactor insulated from the chamber face walls with the buffer gas was demonstrated experimentally and supported by numerical modeling. A decreased temperature of the near-wall gas mixture indicates that the reaction zone is insulated also from other reactor walls. Ethylene was shown to be an efficient converter of laser energy to heat power at ethane pyrolysis.

Thus, ethane pyrolysis was performed in the mode of 'energetic catalysis', where energy absorption for endothermic reaction increased with increasing content of the reaction products. In the process, ethane conversion attained 80% at ethylene yield of 43%. As ethane conversion decreased to 70%, ethylene yield increased to 56%. Effective laser energy absorption in reaction zone was from 30% to 70% of total laser energy.

Acknowledgements

This work was supported by the Russian Foundation for Basic Research (grant no. 08-01-00615, 09-07-00023), SB RAS Integration Project No.26 and Presidium RAN Programmes "Biosphere Origin and Evolution".

References

[1] H. Gladdish, How Huels makes acetylene by DC arc, Pet. Ref. 41 (1962) 159.
[2] G. Zhao, S. John, J. Zhang, L. Wang, S. Muknahallipatna, J. Hamann, J. Ackerman, M. Argyle, O. Plumb, Methane conversion in pulsed corona discharge reactors, Chem. Eng. J. 125 (2) (2006) 67–79.
[3] K. Onoe, A. Fujie, T. Yamaguchi, Y. Hatano, Selective synthesis of acetylene from methane by microwave plasma reactions, Fuel 76 (3) (1997) 281–282.
[4] M. Heintze, M. Magureanu, Methane conversion into aromatics in a direct plasma-catalytic process, J. Appl. Phys. 92 (5) (2002) 2276–2283.
[5] T.P. Forbath, B.J. Gaffney, Acetylene by the BASF process, Pet. Ref. 33 (1954) 160–165.
[6] M.J.P. Bogart, R.H. Long, Pyrolysis of liquid hydrocarbons via the Wulff process, Chem. Eng. Prog. 58 (1962) 91.
[7] G. Pratt, D. Rogers, J. Chem. Soc. 5 (1979) 1089–1100.
[8] A. Holmen, O. Olsvik, O.A. Rokstad, Pyrolysis of natural gas: chemistry and process concepts, Fuel Process. Technol. Pyrol. 42 (1995) 249–267.
[9] F. Billaud, F. Baronnet, Thermal coupling of methane in a tubular flow reactor: parametric study, Ind. Eng. Chem. Res. 32 (1993) 1549–1554.
[10] G. Egloff, The decomposition of the paraffin hydrocarbons, J. Phys. Chem. 34 (1930) 1617.
[11] H.H. Storch, Acetylene formation in thermal decomposition of hydrocarbons, Ind. Eng. Chem. 26 (1934) 56.
[12] M.S. Khan, B.L. Crynes, Survey of recent methane pyrolysis literature, Ind. Eng. Chem. 62 (1970) 54.
[13] K.I. Omar, The pyrolysis of methane, Chem. Eng. Res. Bull. 6 (1982) 29.
[14] F. Billaud, F. Baronnet, E. Freund, C. Busson, J. Weill, Thermal decomposition of methane bibliographic study and proposal of a mechanism, Revue De L Institut Francais Du Petrole, 44, 1989, 813–823.
[15] A. Schuck, H.-R. Volpp, J. Wolfrum, Kinetic investigation of the reactions of NCO radicals with alkanes in the temperature range 294 to 1113 K, Combust. Flame. 99 (3–4) (1994) 491–498.
[16] Tsuboi, Takao, Inomata, Katsumi, Tsunoda, Yutaka, Isobe, Akihito, Nagaya, Kohichi, Jpn. J. Appl. Phys., Part 1: Regular Papers & Short Notes, 24 (1) (1985), 8–13.
[17] M.T. Swihart, R.W. Carr, Pulsed laser powered homogeneous pyrolysis: a computational analysis, Int. J. Chem. Kinet. 26 (8) (1994) 779–799.
[18] A.S. Grady, R.E. Linney, R.D. Markwell, G.P. Mills, D.K. Russell, P.J. Williams, A.C. Jones, Laser-powered homogeneous pyrolysis of triisobutylgallane and tri-tert-butylgallane, J. Mater. Chem. 2 (5) (1992) 539–543.
[19] P.R. Buerki, S. Leutwyler, Substrate-free gas-phase synthesis of diamond powder by CO_2laser pyrolysis of C_2H_4, Surf. Coat. Technol. 47 (1–3) (1991) 22–28.
[20] A. Gupta, T.J. Yardley, Proc. SPIE—Int. Soc. Opt. Eng. 458 (1984) 131–139.
[21] R.L. Woodin, K.A. Kajkowski, Proc. SPIE—Int. Soc. Opt. Eng. 458 (1984) 28–34.
[22] Pola, CO_2 laser-induced thermal chemical vapour deposition of polymers, J. Anal. Appl. Pyrol. 30 (1) (1994), 73–90.
[23] P.R. Buerki, S. Leutwyler, CO_2 laser induced gas-phase synthesis of micron-sized diamond powders, Diamond Relat. Mater. 2 (2–4 pt 1) (1993) 174–182.
[24] P. Engst, J. Pola, M. Horak, Collect. Czech. Chem. Commun. 44 (1979) 406.
[25] J. Pola, P. Engst, M. Horak, Collect. Czech. Chem. Commun. 44 (1979) 2092.
[26] J. Pola, T. Vitlk, M. Horak, P. Engst, Collect. Czech. Chem. Commun. 45 (1980) 1805.
[27] K. Dathe, P. Engst, M. Horak, Collect. Czech. Chem. Commun. (1910) 45.
[28] S. Ruschin, S.H. Bauer, Oscillating convective effects in sulfur hexafluoride-argon laser-heated mixtures, J. Phys. Chem. 88 (1984) 5042.
[29] W.M. Shaub, S.H. Bauer, Laser-powered homogeneous pyrolysis, Int. J. Chem. Kinet. 7 (1975) 509.
[30] FLUENT, http://www.fluent.com.
[31] G.K. Batchelor, An Introduction to Fluid Dynamics, Cambridge Univ. Press, Cambridge, England, 1967.
[32] C. Riverol, M.V. Pilipovik, Optimization of the pyrolysis of ethane using fuzzy programming, Chem. Eng. J. 133 (1–3) (2007) 133–137.
[33] C.P. Quinn, The thermal dissociation and pyrolysis of ethane, Proc. Royal Soc. Lond. Ser. A, Math. Phys. Sci. 275 (1361) (1963) 190–199.
[34] Ethane pyrolysis, British patent No. 1335892 (1996).
[35] O.B. Braginsky, Validation of choice of direction of scientific progress in petrochemical industry, M. Neftechim. 21 (1985) (in Russian).
[36] S. Hou, Y. Cao, W. Xiong, H. Liu, Y. Kou, Site requirements for the oxidative coupling of methane on SiO_2-supported Mn catalysts, Ind. Eng. Chem. Res. 45 (21) (2006) 7077–7083.
[37] J. Wang, L. Chou, B. Zhang, H. Song, J. Zhao, J. Yang, S.J. Li, La-promoted Na_2WO_4/Mn/SiO_2 catalysts for the oxidative conversion of methane simultaneously to ethylene and carbon monoxide. Comparative study on oxidation of methane to ethane and ethylene over Na_2WO_4–Mn/SiO_2 catalysts prepared by different methods, Mol. Catal. A: Chem. 245 (1–2) (2006) 272–277.
[38] J. Wu, H. Zhang, S. Qin, C. Hu, Study of the effect of gas space time on the combination of methane gas-phase oxidation and catalytic oxidative coupling over Mn/Na_2WO_4/SiO_2 catalyst, Appl. Catal. A: Gen. 323 (2007) 126–134.
[39] H. Zhang, J. Wu, S. Qin, C. Hu, Spectroscopic and kinetic analysis of a new low-temperature methanol synthesis reaction, Ind. Eng. Chem. Res. 45 (21) (2006) 7090–7095.

[40] H. Zhang, J. Wu, B. Xu, C. Hu, Dual catalyst bed for the oxidation of CH_4 simultaneously to C_2H_4 and syngas, Catal. Lett. 106 (3–4) (2006) 161–165.
[41] C. Hu, J. Wu, H. Zhang, S. Qin, Oxidative coupling of methane over lithium doped (Mn+W)/SiO_2 catalysts, AIChE J. 53 (11) (2007) 2925–2931.
[42] A. Malekzadeh, A. Khodadadi, A.K. Dalai, M.J. Abedini, Process optimization of oxidative coupling of methane for ethylene production using response surface methodology, Natural Gas Chem. 16 (2) (2007) 121–129.
[43] C.Y. Thien, A.R. Mohamed, S.J. Bhatia, Structural features of Na_2WO_4–MO_x/$SiOP_2$ catalyst in oxidative coupling of methane reaction, Chem. Technol. Biotechnol. 82 (1) (2007) 81–91.
[44] A. Malekzadeh, A.K. Dalai, A. Khodadai, Y. Mortazavi, Get smarter by sharing ideas, Catal. Commun. 9 (2008) 960–965.
[45] D. Knott, Oil Gas J. 105 (35) (1997) 17.
[46] P. Schmalfeld, Hydroc. Proc. 42 (7) (1963) 145–148.